5.1 Geometrical Synthesis of Inductively-Compensated Multi-Stage Amplifiers - A Simple Example

The reader who has patiently followed the discussion presented in previous chapters is probably eager to see all that theory being put into practice.

Before jumping to some more complex amplifier circuits, we will give a relatively simple example of a two-stage differential cascode amplifier, by which we will illustrate the actual system optimization procedure in some detail, using the previously developed principles in their full potential.

Since we want to grasp the "big picture", we will have to leave out some less important topics, such as the negative input impedance compensation, the cascode damping, etc. These are important for the optimization of each particular stage, which, once optimized, can be idealized to some extent. We have covered that extensively enough in Part 3, so we will not explicitly draw the associated components in the schematic diagram. But, at the end of our calculations, we will briefly discuss the influence of those components to final circuit values.

A two-stage amplifier is a "minimum complexity" system for which the multistage design principles still apply. To this, we will add a 3-pole T-coil and a 4-pole L+T-coil peaking networks, discussed in Part 2, as loads to each stage, making a total of 7 poles. There is, however, an additional real pole, due to the Q_1 input capacitance and the total input and signal source resistance. As we will see later, this pole can be neglected if its distance from the complex-plane origin is at least twice as large as that of the system real pole set by $-1/R_{\mathrm{a}}C_{\mathrm{a}}$.

Such an amplifier thus represents an elementary example, in which everything that we have learned so far can be applied. The reader should, however, be aware that this is by no means the ideal or, worse still, the only possibility. At the end of our calculations, when we will be able to assess the advantages and limitations offered by our initial choices at each stage, we will examine a few possibilities for further improvement.

We will start our calculations from the unavoidable stray capacitances and the desired total voltage gain. Then, we will apply an optimization process, which we like to refer to as the **geometrical synthesis**, by which we will calculate all the remaining circuit components in such a way, that the resulting system will conform to the 7-pole normalized Bessel-Thomson system. The only difference will be that the actual amplifier poles will be larger by a certain factor, proportional (but not equal) to the upper half-power frequency, ω_{H}. We have already met the geometrical synthesis in its basic form in Part 2, Fig. 2.5.3 when we were discussing the 3-pole T-coil circuit. The name springs from the fact that, for a given pole pattern and a few independent component values, the remaining components can be calculated from simple geometrical relations, involving the pole real an imaginary components. Here we are going to see a generalization of those basic relations, applied to the whole amplifier.

We must admit that the constant and real input impedance of the T-coil network is the main factor which allows us to assign so many poles to only two stages. Actually, we could use a cascade of passive two-pole sections, but they would load each other and, as a result, the bandwidth extension factor would suffer. Another possibility would be to use an additional cascode stage to separate the last two

peaking sections, but another active stage, while adding gain, adds also its own problems to take care of. It is, nevertheless, a perfectly valid option.

Let's take now a quick tour of the amplifier schematic, Fig. 5.1.1. We have two differential cascode stages and two current sources, which set both the transistor transconductance and the maximum current available to load resistors, R_a and R_b. This limits the voltage range available to the CRT. Since the circuit is differential, the total gain is a double of each half. The total d.c. gain is (approximately) :

$$A_{dc} = 2\,\frac{R_a}{R_{e1}} \cdot \frac{R_b}{R_{e2}} \tag{5.1.1}$$

The values of R_{e1} and R_{e2} set the required capacitive bypass, $C_{e1}/2$ and $C_{e3}/2$, to match the transistor time-constants. In turn, this sets the input capacitance at the base of Q_1 and Q_3, to which we must add the inevitable C_{cb} and some strays.

The capacitance C_d should thus consists of, preferably, only the input capacitance at the base of Q_3. If required by the coil tuning, it can easily be increased by adding a small capacitance in parallel. Note that the associated T-coil, L_d, will have to be designed as an interstage peaking, as discussed in Part 3, Sec. 3.6, but we can leave the necessary corrections to be done at the end.

The capacitance C_b, due almost entirely to the CRT vertical plates, is much larger than C_d, so we expect that R_a and R_b can not be equal. From this it follows that it might be difficult to apply equal gain to each stage, in accordance with the principle explained in Part 4, Eq. 4.1.39. Nevertheless, the difference in gain will not be too high, as we shall see.

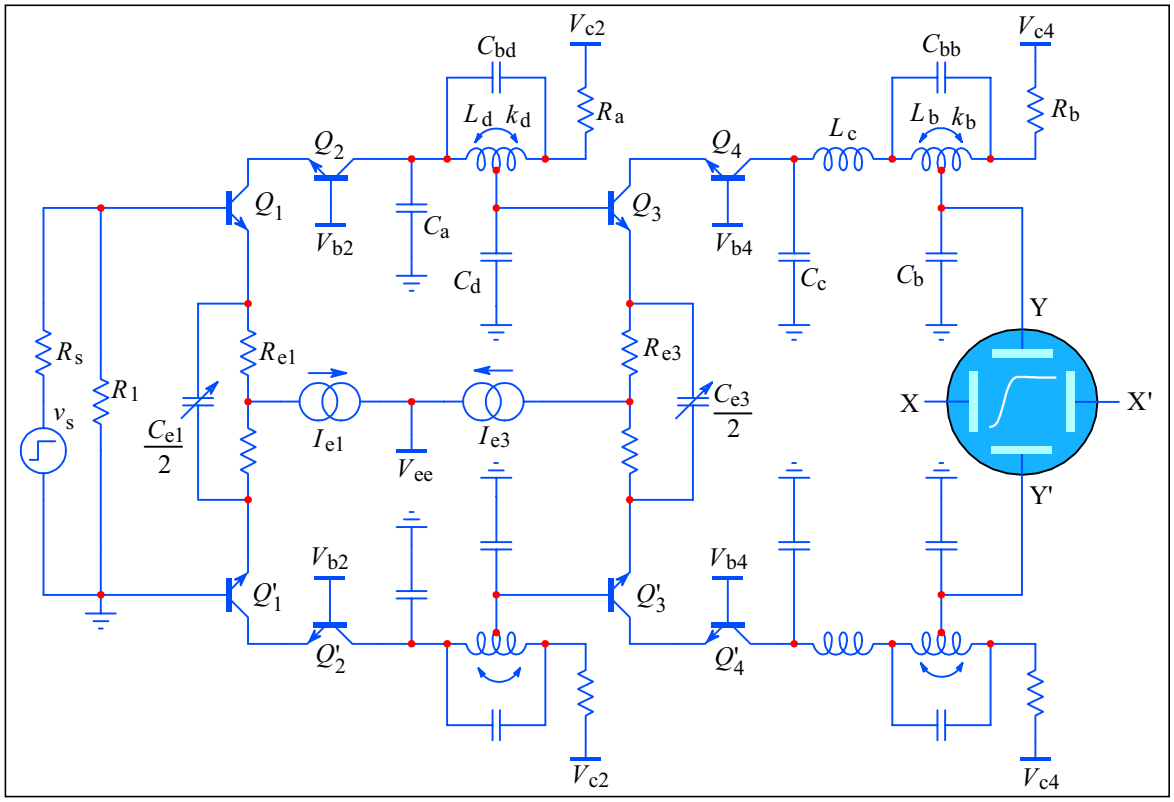

Fig. 5.1.1 : A simple 2-stage differential cascode amplifier with a 7-pole peaking system : the 3-pole T-coil interstage peaking (between the Q_2 collector and the Q_3 base) and the 4-pole L+T-coil output peaking (between the Q_4 collector and the vertical plates of the cathode-ray tube). The schematic was simplified to emphasize the important design aspects - see text.

Like any other engineering process, the geometrical synthesis also starts from some external boundary conditions, which set the main design goal. In this case, it is the CRT vertical sensitivity and the available input voltage, from which the total gain is defined. The next condition is the choice of transistors, by which the available current is defined. Both the CRT and the transistors set the lower limit of the loading capacitances at various nodes. From these, the first circuit component R_b is fixed.

With R_b fixed, we arrive at the first "free" parameter, which can be represented by several circuit components. However, since we would like to maximize the bandwidth, this parameter should be attributed to one of the capacitances. By comparing the design equations for the 3-pole T-coil and the 4-pole L+T-coil peaking networks in Part 2, it can be deduced that C_a, the input capacitance of the 3-pole section, is the most critical component.

With these boundaries set, let's say that we have the following component values to start the design :

$C_b = 11\,\text{pF}$ (9 pF of the CRT vertical plates, 2 pF stray)

$C_a = 4\,\text{pF}$ (3 pF from the Q_2 C_{cb} , 1 pF stray)

$R_b = 360\ \Omega$ (5.1.2)

The pole pattern is, in the general case, also a "free" parameter, but we would like to have a nice smooth transient, so we have no other choice but to adopt the Bessel-Thomson pattern. As can be seen in Fig. 5.1.2, each pole (-pair) defines a circle going through the pole and the origin and with the center on the negative real axis.

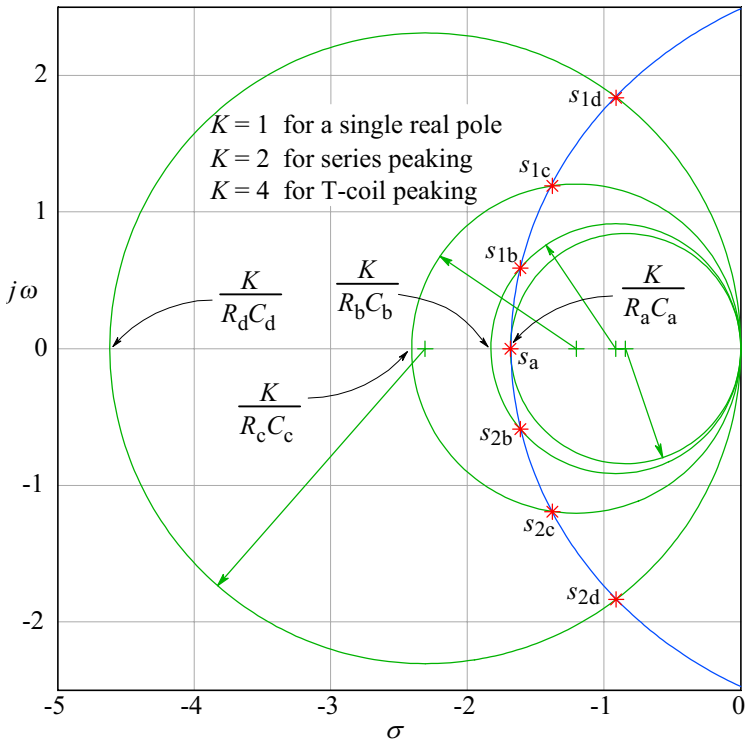

Fig. 5.1.2 : The 7 Bessel-Thomson poles. The characteristic circle of each pole (-pair) has a diameter defined by the appropriate RC-constant and the peaking factor K, which depends on the type of network chosen.

The poles in Fig. 5.1.2 bear the index of the associated circuit components and the reader might wonder why we have chosen precisely that assignment.

In a general case, the assignment of a pole (-pair) to a particular circuit section is yet another "free" design parameter. If we were designing a low-frequency filter, we could indeed have chosen an arbitrary assignment (as long as each complex-conjugate pole-pair is assigned as a pair, a limitation due to physics, instead of circuit theory).

If, however, the bandwidth is an issue, then we must seek those nodes with the largest capacitances and apply the poles with the lowest imaginary part to those circuit sections. This is because the capacitor impedance (which is dominantly imaginary) is inversely proportional both to the capacitor value and the signal frequency.

In this light, the largest capacitance is at the CRT, that is C_b; thus the pole-pair with the lowest imaginary part is assigned to the output T-coil section, formed by L_b and R_b, therefore acquiring the index "b", $s_{1\mathrm{b}}$ and $s_{2\mathrm{b}}$.

The real pole is the one associated with the 3-pole stage and there it is set by the loading resistor R_a and the input capacitance C_a, becoming s_a.

The remaining two pole pairs should be assigned so that the pair with the larger imaginary part is applied to that peaking network which has a larger bandwidth improvement factor. Here we must consider that, for a T-coil, $K = 4$ and for the series-peaking L-section (of the 4-pole L+T-scetion) $K = 2$. Clearly, the pole-pair with the larger imaginary part should be assigned to the interstage T-coil, L_d, thus they are labeled $s_{1\mathrm{d}}$ and $s_{2\mathrm{d}}$. The L-section then gets the remaining pair, $s_{1\mathrm{c}}$ and $s_{2\mathrm{c}}$.

We have thus arrived at a solution which seems logical, but in order to be sure that we have made the right choice, we should check other combinations, as well. We are going to do it at the end of the design process.

The poles for the normalized 7th-order Bessel-Thomson system, as taken either from Part 4, Table 4.4.3, or by using the BESTAP (Part 6) routine, along with the associated angles, are :

$$\begin{aligned}
s_\mathrm{a} = \sigma_\mathrm{a} &= -4.9718 & \theta_\mathrm{a} &= 180° \\
s_\mathrm{b} = \sigma_\mathrm{b} \pm j\,\omega_\mathrm{b} &= -4.7583 \pm j\,1.7393 & \theta_\mathrm{b} &= 180° \mp 20.0787° \\
s_\mathrm{c} = \sigma_\mathrm{c} \pm j\,\omega_\mathrm{c} &= -4.0701 \pm j\,3.5172 & \theta_\mathrm{c} &= 180° \mp 40.8316° \\
s_\mathrm{d} = \sigma_\mathrm{d} \pm j\,\omega_\mathrm{d} &= -2.6857 \pm j\,5.4207 & \theta_\mathrm{d} &= 180° \mp 63.6439°
\end{aligned} \qquad (5.1.3)$$

So, let us now express the basic design equations from the assigned poles and the components of the two peaking networks.

For the real pole s_a we have the following familiar proportionality :

$$s_\mathrm{a} = \sigma_\mathrm{a} = D_\mathrm{a} = -4.9718 \quad \propto \quad -\frac{1}{R_\mathrm{a}\,C_\mathrm{a}} \qquad (5.1.4)$$

At the output T-coil section, we have, according to Part 2, Fig. 2.5.3 :

$$D_\mathrm{b} = \frac{\sigma_\mathrm{b}}{\cos^2\theta_\mathrm{b}} = \frac{-4.7583}{0.8821} = -5.3941 \quad \propto \quad -\frac{4}{R_\mathrm{b}\,C_\mathrm{b}} \qquad (5.1.5)$$

For the L-section of the output L+T network, due to the fact that the T-coil input impedance is equal to the loading resistor, we have :

$$D_\mathrm{c} = \frac{\sigma_\mathrm{c}}{\cos^2\theta_\mathrm{c}} = \frac{-4.0701}{0.5725} = -7.1094 \quad \propto \quad -\frac{2}{R_\mathrm{b}\,C_\mathrm{c}} \qquad (5.1.6)$$

And finally, for the interstage T-coil network :

$$D_d = \frac{\sigma_d}{\cos^2\theta_d} = \frac{-2.6857}{0.1917} = -13.6333 \quad \propto \quad -\frac{4}{R_a\,C_d} \tag{5.1.7}$$

From these equations we can calculate the required values of the remaining capacitances, C_c and C_d . If we divide Eq. 5.1.5 by Eq. 5.1.6, we have the ratio :

$$\frac{D_b}{D_c} = \frac{-\dfrac{4}{R_b\,C_b}}{-\dfrac{2}{R_b\,C_c}} = \frac{2\,C_c}{C_b} \tag{5.1.8}$$

It follows that the capacitance C_c should be :

$$C_c = \frac{C_b}{2}\cdot\frac{D_b}{D_c} = \frac{11}{2}\cdot\frac{-5.3941}{-7.1094} = 4.1730\,\text{pF} \tag{5.1.9}$$

Likewise, if we divide Eq. 5.1.4 by Eq. 5.1.7, we get :

$$\frac{D_a}{D_d} = \frac{-\dfrac{1}{R_a\,C_a}}{-\dfrac{4}{R_a\,C_d}} = \frac{C_d}{4\,C_a} \tag{5.1.10}$$

Thus C_d will be :

$$C_d = 4\,C_a\,\frac{D_a}{D_d} = 4\cdot 4\cdot\frac{-4.9718}{-13.6333} = 5.8349\,\text{pF} \tag{5.1.11}$$

Of course, for most practical purposes, the capacitances don't need to be calculated to such precision, a resolution of 0.1 pF should be more than enough. But we would like to check our procedure by recalculating the actual poles from circuit components and for that purpose we will need this precision.

Now we need to know the value of R_a . This can be readily calculated from the ratio D_a/D_b :

$$\frac{D_a}{D_b} = \frac{-\dfrac{1}{R_a\,C_a}}{-\dfrac{4}{R_b\,C_b}} = \frac{R_b\,C_b}{4\,R_a\,C_a} \tag{5.1.12}$$

resulting in :

$$R_a = \frac{R_b}{4}\cdot\frac{C_b}{C_a}\cdot\frac{D_b}{D_a} = \frac{360}{4}\cdot\frac{11}{4}\cdot\frac{-5.3941}{-4.9718} = 268.5\,\Omega \tag{5.1.13}$$

We are now ready to calculate the inductances L_b, L_c and L_d. For the two T-coils we can use the Eq. 2.4.19 :

$$L_b = R_b^2\,C_b = 360^2\cdot 11\cdot 10^{-12} = 1.4256\,\mu\text{H} \tag{5.1.14}$$

and

$$L_d = R_a^2\,C_d = 268.5^2\cdot 5.8349\cdot 10^{-12} = 0.4206\,\mu\text{H} \tag{5.1.15}$$

For L_c we use Eq. 2.2.26 to get the proportionality factor :

$$L_c = \frac{1+\tan^2\theta_b}{4} R_b^2 C_c = \frac{360^2 \cdot 4.1730 \cdot 10^{-12}}{4 \cdot 0.8821} = 0.1533\,\mu\text{H} \qquad (5.1.16)$$

The magnetic coupling factors for the two T-coils are calculated by Eq. 2.4.36 :

$$k_b = \frac{3-\tan^2\theta_b}{5+\tan^2\theta_b} = \frac{3-0.1336}{5+0.1336} = 0.5584 \qquad (5.1.17)$$

and likewise :

$$k_d = \frac{3-\tan^2\theta_d}{5+\tan^2\theta_d} = \frac{3-4.0738}{5+4.738} = -0.1183 \qquad (5.1.18)$$

Note that k_d is negative. This means that, instead of the usually negative mutual inductance, we will need a positive inductance at the T-coil tap. This can be achieved by simply mounting the two halves of L_d perpendicular to each other, in order to have zero magnetic coupling and then introduce an additional coil, L_e, again perpendicular to both halves of L_d, with a value of the required positive mutual inductance, as can be seen in Fig. 5.1.3. Another possibility would be to wind the two halves of L_d in opposite direction, but then the bridge capacitance C_{bd} might be difficult to realize correctly.

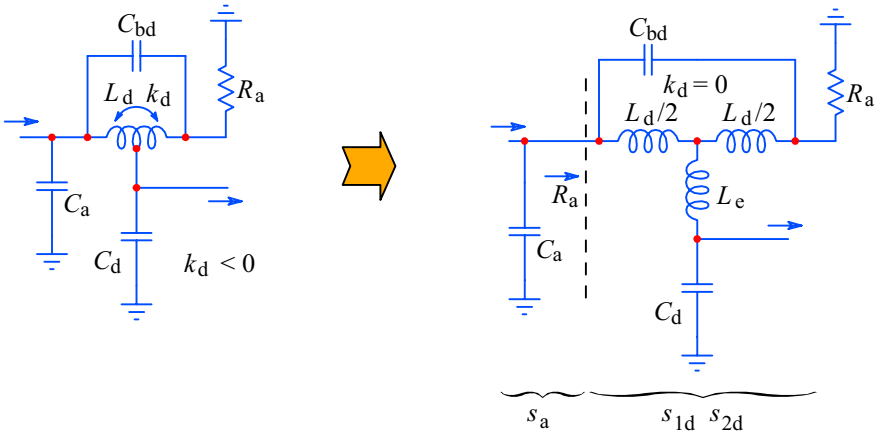

Fig. 5.1.3 : The 3-pole stage has the magnetic coupling k_d negative, which forces us to use non-coupled coils and add a positive mutual inductance L_e. The T-coil reflects its resistive load to the network input, greatly simplifying the calculations of component values.

The additional inductance L_e is calculated from the required mutual inductance given by the negative value of k_d. In Part 2 (Eq. 2.4.1-2.4.5), we have defined the T-coil inductance and its components by :

$$L = L_1 + L_2 + 2\,M$$

$$L_1 = L_2 = \frac{L}{2\,(1+k)}$$

$$M = -\,k\,\sqrt{L_1\,L_2} \qquad (5.1.19)$$

thus, if $k = 0$:

$$L_{1d} = L_{2d} = \frac{L_d}{2} = \frac{0.4206}{2} = 0.2103\,\mu\text{H} \tag{5.1.20}$$

and :

$$L_e = -k_d \sqrt{\frac{L_d}{2} \cdot \frac{L_d}{2}} = -k_d \frac{L_d}{2} = 0.1183 \frac{0.4206}{2} = 0.025\,\mu\text{H} \tag{5.1.21}$$

If we would account for the Q_3 base resistance, as we discussed in Part 3, we would get k_d even more negative and the coil tap would not be centered any more.

The coupling factor k_b , although positive, also poses a problem : since it is greater than 0.5, it might be difficult to realize. As can be noted from the above equations, the value of k depends only of the pole angle θ. In fact, the 2 nd-order Bessel system has the pole angles of $\pm 150°$, resulting in a $k = 0.5$, representing the limiting case of realizability with conventionally wounded coils. Special shapes, coil overlapping, or other exotic techniques may solve the coupling problem, but, more often than not, they will also impair the bridge capacitance. The other limiting case, when $k = 0$, is reached by the ratio $\Im\{s\}/\Re\{s\} = \sqrt{3}$, a situation occurring when the pole angle $\theta = 120°$.

In accordance with previous equations, we also calculate the value of the two halves of L_b :

$$L_{1b} = L_{2b} = \frac{L_b}{2\,(1 + k_b)} = \frac{1.4256}{2\,(1 + 0.5584)} = 0.4574\,\mu\text{H} \tag{5.1.22}$$

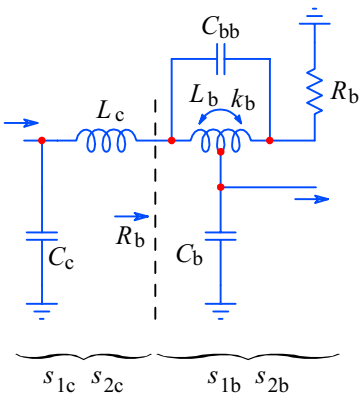

Fig. 5.1.4 : The 4-pole output L+T-coil stage and its pole assignment.

The last components to be calculated are the bridge capacitances, C_{bb} and C_{bd} . The relation between the T-coil loading capacitance and the bridge capacitance was given already in Eq. 2.4.31 , thus we will have the following expressions :

$$C_{bb} = C_b \frac{1 + \tan^2 \theta_b}{16} = 11 \frac{1 + 0.1336}{16} = 0.7793\,\text{pF} \tag{5.1.23}$$

and :

$$C_{bd} = C_d \frac{1 + \tan^2 \theta_d}{16} = 5.8349 \frac{1 + 4.0738}{16} = 1.8503\,\text{pF} \tag{5.1.24}$$

This completes the calculation of amplifier components necessary for the inductive-peaking compensation and thus achieving the Bessel-Thomson system response. We would now like to verify the design by recalculating the actual pole values. To do this we return to the relations which we have started from, Eq. 5.1.3 to Eq. 5.1.7 and for the imaginary part using the relations in Part 2, Fig. 2.5.3 . In order not to confuse the actual pole values with the normalized values, from which we started, we add an index "A" to the actual poles :

$$\sigma_{aA} = -\frac{1}{R_a\,C_a} = \frac{1}{268.5 \cdot 4 \cdot 10^{-12}} = -931.1 \cdot 10^6\ \text{rad/s}$$

$$\sigma_{bA} = -\frac{4\cos^2\theta_b}{R_b\,C_b} = \frac{4 \cdot 0.8821}{360 \cdot 11 \cdot 10^{-12}} = -891.0 \cdot 10^6\ \text{rad/s}$$

$$\omega_{bA} = \pm\frac{4\cos\theta_b \sin\theta_b}{R_b\,C_b} = \pm\frac{4 \cdot 0.9392 \cdot 0.3433}{360 \cdot 11 \cdot 10^{-12}} = \pm 325.7 \cdot 10^6\ \text{rad/s}$$

$$\sigma_{cA} = -\frac{2\cos^2\theta_c}{R_b\,C_c} = \frac{2 \cdot 0.5725}{360 \cdot 4.1730 \cdot 10^{-12}} = -762.2 \cdot 10^6\ \text{rad/s}$$

$$\omega_{cA} = \pm\frac{2\cos\theta_c \sin\theta_c}{R_b\,C_c} = \pm\frac{2 \cdot 0.7566 \cdot 0.6538}{360 \cdot 4.1730 \cdot 10^{-12}} = \pm 658.5 \cdot 10^6\ \text{rad/s}$$

$$\sigma_{dA} = -\frac{4\cos^2\theta_d}{R_a\,C_d} = \frac{4 \cdot 0.1917}{268.5 \cdot 5.8349 \cdot 10^{-12}} = -489.5 \cdot 10^6\ \text{rad/s}$$

$$\omega_{dA} = \pm\frac{4\cos\theta_d \sin\theta_d}{R_a\,C_d} = \pm\frac{4 \cdot 0.4439 \cdot 0.8961}{268.5 \cdot 5.8349 \cdot 10^{-12}} = \pm 1015.6 \cdot 10^6\ \text{rad/s} \qquad (5.1.25)$$

If we divide the real amplifier pole by the real normalized pole, we get :

$$\frac{\sigma_{bA}}{\sigma_b} = \frac{-931.1 \cdot 10^6}{-4.9718} = 187.3 \cdot 10^6 \qquad (5.1.26)$$

and this factor is equal for all other pole components. Unfortunately, from this we cannot calculate the upper half-power frequency of the amplifier. The only way to do it (for a Bessel system) is to calculate the response for a range of frequencies and then iterate it using the bisection method, until a satisfactory tolerance has been achieved.

Instead of doing it for only a small range of frequencies, we will rather do it for a three decade range and compare the resulting response with the one we would get from a non-compensated amplifier (in which all the inductances are zero). Since we were not interested in the actual value of the voltage gain, we will make the comparison using amplitude-normalized responses.

The non-compensated amplifier has two real poles, which are :

$$s_{1N} = -\frac{1}{R_a\,(C_a + C_d)} \quad \text{and} \quad s_{2N} = -\frac{1}{R_b\,(C_b + C_c)} \qquad (5.1.27)$$

The non-compensated complex-frequency response would then be :

$$F_{\mathrm{N}}(s) = \frac{s_{1\mathrm{N}}\, s_{2\mathrm{N}}}{(s - s_{1\mathrm{N}})(s - s_{2\mathrm{N}})} \tag{5.1.28}$$

with the magnitude :

$$\left|F_{\mathrm{N}}(\omega)\right| = \frac{\sqrt{s_{1\mathrm{N}}\, s_{2\mathrm{N}}}}{\sqrt{(\omega^2 - s_{1\mathrm{N}}^2)(\omega^2 - s_{2\mathrm{N}}^2)}} \tag{5.1.29}$$

and the step-response :

$$\begin{aligned} g(t) &= \mathcal{L}^{-1}\left\{ \frac{s_{1\mathrm{N}}\, s_{2\mathrm{N}}}{s\,(s - s_{1\mathrm{N}})(s - s_{2\mathrm{N}})} \right\} \\ &= 1 + \frac{s_{2\mathrm{N}}}{s_{1\mathrm{N}} - s_{2\mathrm{N}}}\, \mathrm{e}^{s_{1\mathrm{N}} t} - \frac{s_{1\mathrm{N}}}{s_{1\mathrm{N}} - s_{2\mathrm{N}}}\, \mathrm{e}^{s_{2\mathrm{N}} t} \end{aligned} \tag{5.1.30}$$

The risetime is :

$$\tau_{\mathrm{r}} = 2.2 \sqrt{\frac{1}{s_{1\mathrm{N}}^2} + \frac{1}{s_{2\mathrm{N}}^2}} \tag{5.1.31}$$

and the half-power frequency :

$$f_{\mathrm{h}} = \frac{\sqrt{s_{1\mathrm{N}}\, s_{2\mathrm{N}}}}{2\,\pi} \tag{5.1.32}$$

The 7-pole amplifier has its complex-frequency response :

$$F_{\mathrm{A}}(s) = A_0\, \frac{-\, s_{\mathrm{aA}}\, s_{1\mathrm{bA}}\, s_{2\mathrm{bA}}\, s_{1\mathrm{cA}}\, s_{2\mathrm{cA}}\, s_{1\mathrm{dA}}\, s_{2\mathrm{cA}}}{(s - s_{\mathrm{aA}})(s - s_{1\mathrm{bA}})(s - s_{2\mathrm{bA}})(s - s_{1\mathrm{cA}})(s - s_{2\mathrm{cA}})(s - s_{1\mathrm{dA}})(s - s_{2\mathrm{dA}})} \tag{5.1.33}$$

and the step-response is the inverse Laplace transform of the product of $F_{\mathrm{A}}(s)$ and the unit-step operator, $1/s$:

$$g(t) = \mathcal{L}^{-1}\left\{ \frac{1}{s}\, F_{\mathrm{A}}(s) \right\} = \sum \mathrm{res}\left(\frac{1}{s}\, F_{\mathrm{A}}(s)\, \mathrm{e}^{st} \right) \tag{5.1.34}$$

We will not attempt to solve either of these functions analytically, since it would take too much space and, anyway, we have solved them separately for its two parts (3rd- and 4th-order) in Part 2. Because the systems are separated by an amplifier (Q_3 , Q_4), the frequency response would be a simple multiplication of the two responses. For the step-response, we now have 8 residues to sum (7 of the system poles, in addition to the one from the unit-step operator). Although lenghty, it is a relatively simple operation and we leave it as an exercise to the reader. Instead, we are going to use the computer routines, the development of which can be found in Part 6.

In Fig. 5.1.5 we have made a polar plot of the poles for the inductively compensated 7-pole system and the non-compensated 2-pole system. As we have learned in Part 1 and Part 2, the farther from origin, the smaller is the pole influence

on the system response. It is therefore obvious that the 2-pole system response will be dominated by the pole closer to the origin and that is the pole of the output stage, s_{2N}. The bandwidth of the 7-pole system is, obviously, much larger.

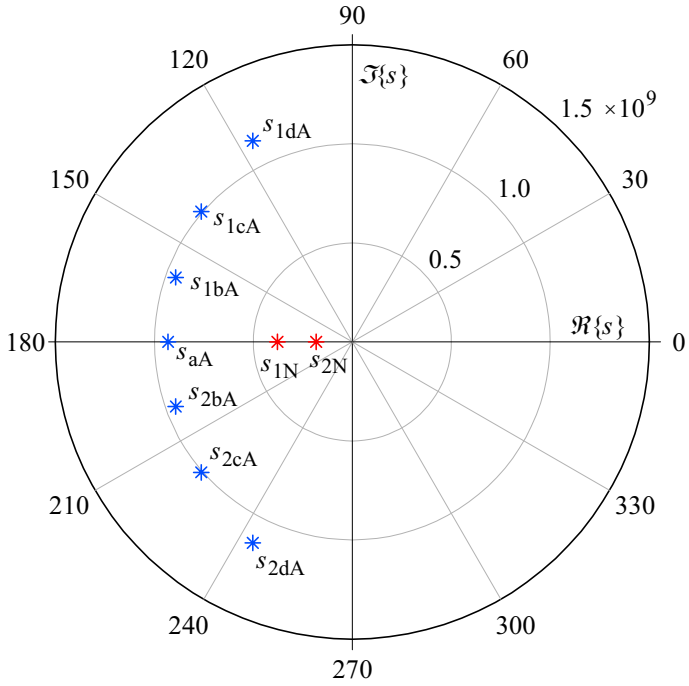

Fig. 5.1.5 : The polar plot of the 7-pole compensated system (poles with index A) and the 2-pole non-compensated system (index N). The radial scale is $\times 10^9$ rad/s. The angle is in degrees.

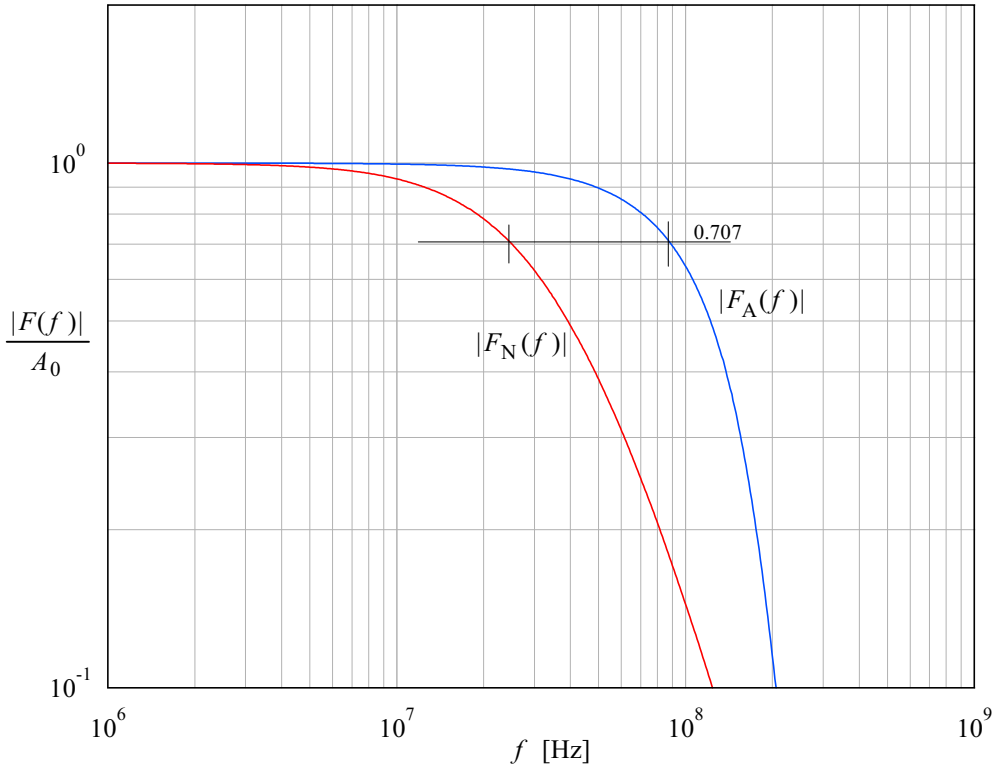

Fig. 5.1.6 : The gain-normalized magnitude vs. frequency of the 7-pole compensated system $|F_A(f)|$ and the 2-pole non-compensated system, $|F_N(f)|$. The bandwidth of F_N is about 25 MHz and the bandwidth of F_A is about 88 MHz, 3.5 times larger.

The pole layout gives just a convenient indication of the system performance, but it is the magnitude vs. frequency response that exposes it clearly. As it can be seen in Fig. 5.1.6, the non-compensated system has a bandwidth of nearly 25 MHz. The compensated amplifier bandwidth is close to 88 MHz, more than 3.5 times larger.

The comparison of step-responses in Fig. 5.1.7 exposes the difference in performance even more dramatically. The risetime of the non-compensated system is about 13.3 ns and for the compensated system it's only 3.8 ns, also a factor of 3.5 times better and with an overshoot of only 0.48 % .

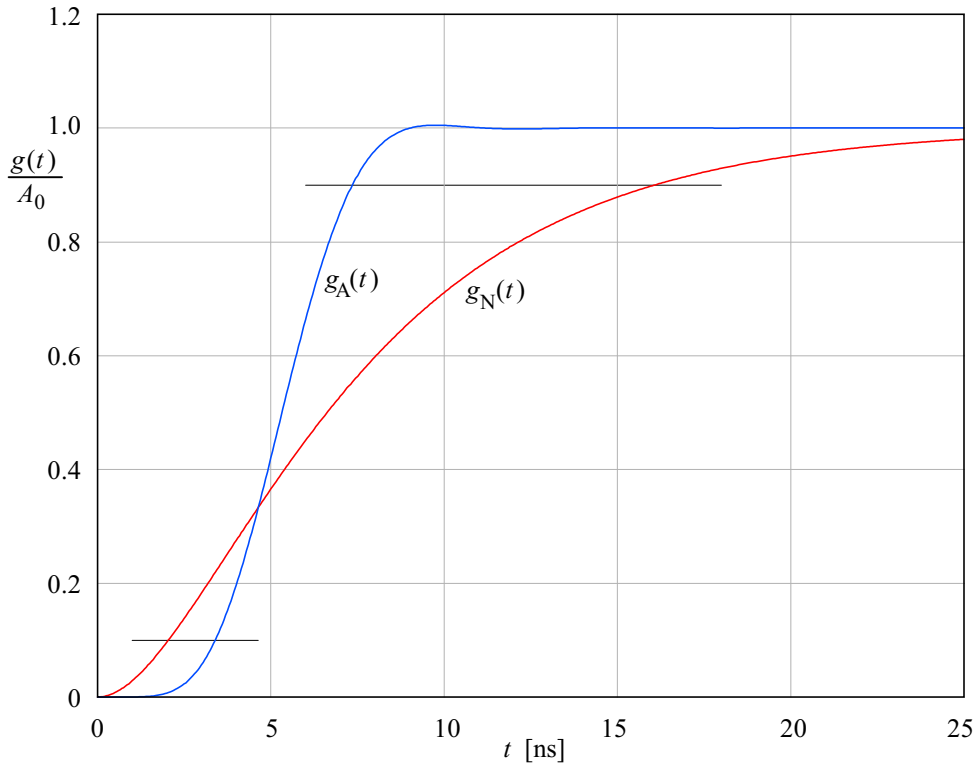

Fig. 5.1.7 : The gain-normalized step-responses of the 7-pole compensated system $g_A(t)$ and the 2-pole non-compensated system $g_N(t)$. The risetimes are 13.3 ns for $g_N(t)$ and only 3.8 ns for $g_A(t)$. The overshoot of $g_A(t)$ is only 0.48 % .

The above comparison of the inductively compensated and the non-compensated amplifier shows an impressive improvement in performance. But, is it the best that could be obtained from this circuit configuration ? After all, in Part 2 we have seen a similar improvement from just the 4-pole L+T-coil section and we expect that the addition of the 3-pole section should yield a slightly better result at least.

One obvious way to extend the bandwidth would be to lower the value of R_b, increase the bias currents and scale the remaining components accordingly. Then we should increase the input signal amplitude to get the same output. But this is the "trivial" solution (mathematically, at least ; not so when building an actual circuit).

By a careful inspection of the amplifier design equations and comparing them with the analysis of the two sections in Part 2, we come to the conclusion that the most serious bandwidth drawback factor is the high value of the CRT capacitance, which is much higher than C_a or C_d. But if so, did we limit the possible improvement by assigning the poles with the lowest imaginary part to the output ? Shouldn't we get a better performance if we add more peaking to the output stage ?

Since we have put the design equations and the response analysis into a computer routine, we can now investigate the effect of different pole assignments. To do so, we simply reorder the poles and run the routine again. Besides the pole order that we have described, let's indicate it by the pole order : abcd (Eq. 5.1.3), we have 5 additional permutations : abdc, acbd, adbc, acdb, adcb. The last two permutations result in a rather slow system, requiring a large inductance for L_b and large capacitances C_c and C_d . But the remaining ones deserve a look.

In Fig. 5.1.8 we have plotted the four normalized step responses and, in order to distinguish them more clearly, we have displaced them vertically by a small offset. This was necessary, since we have two identical pairs of responses and they would be plotted one on top of the other.

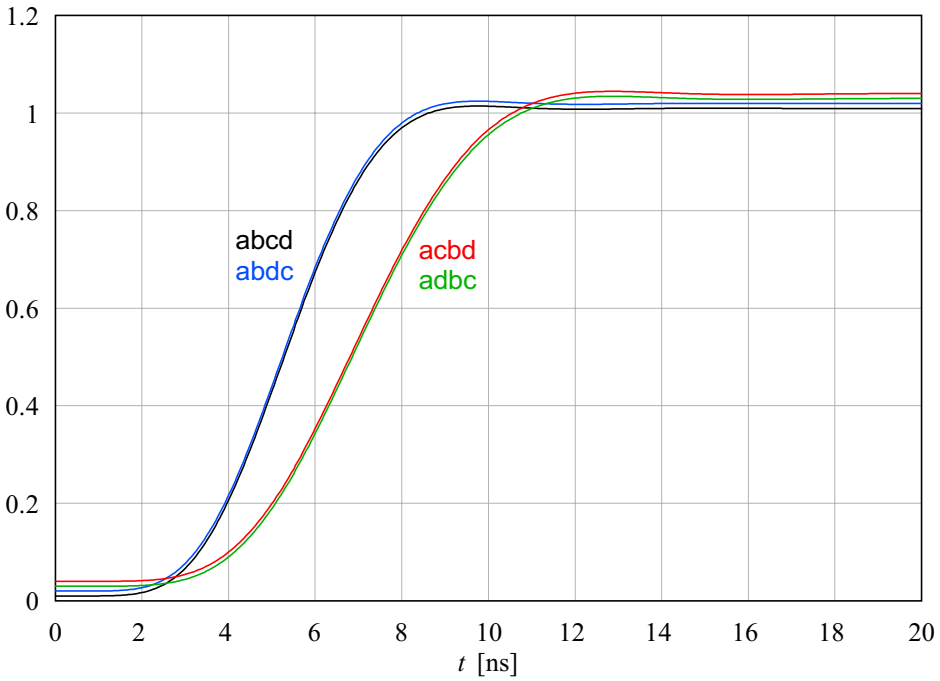

Fig. 5.1.8 : The normalized step responses of all four possible combinations of pole assignments. There are two pairs of responses, here spaced vertically by a small offset to allow easier identifications. The analysis that we have done in detail is one of the faster responses, "abcd" (black).

If the pole-pairs s_c and s_d are mutually exchanged, the result is the same as our original analysis. But, by exchanging s_b with either s_c or s_d , the result is suboptimal.

A closer look at Table 5.1 reveals that both of the slower responses have $R_a = 354\,\Omega$ instead of $268\,\Omega$. The higher value of R_a means actually a higher gain, as can be seen in Fig. 5.1.9, where the original system was set for a gain of $A_0 \approx 10$, in contrast with the higher value, $A_0 \approx 13$. The higher gain results from a different tuning of the 3-pole T-coil stage, in accordance with the different pole assignment.

Since our primary design goal is the bandwidth and not gain, we might try to recalculate the system by lowering the initial value of R_b. If we select a value (from the 0.5 % tolerance E-96 series of standard values) of $316\,\Omega$, the gain will be very close to the original one. This situation is shown in Fig. 5.1.10. The difference between the two system pairs is much smaller, however, the recalculated pair still has a slightly lower bandwidth. This fact nicely illustrates that our initial assumptions of

how to achieve maximum bandwidth (within a given configuration) were not guessed out of sheer luck.

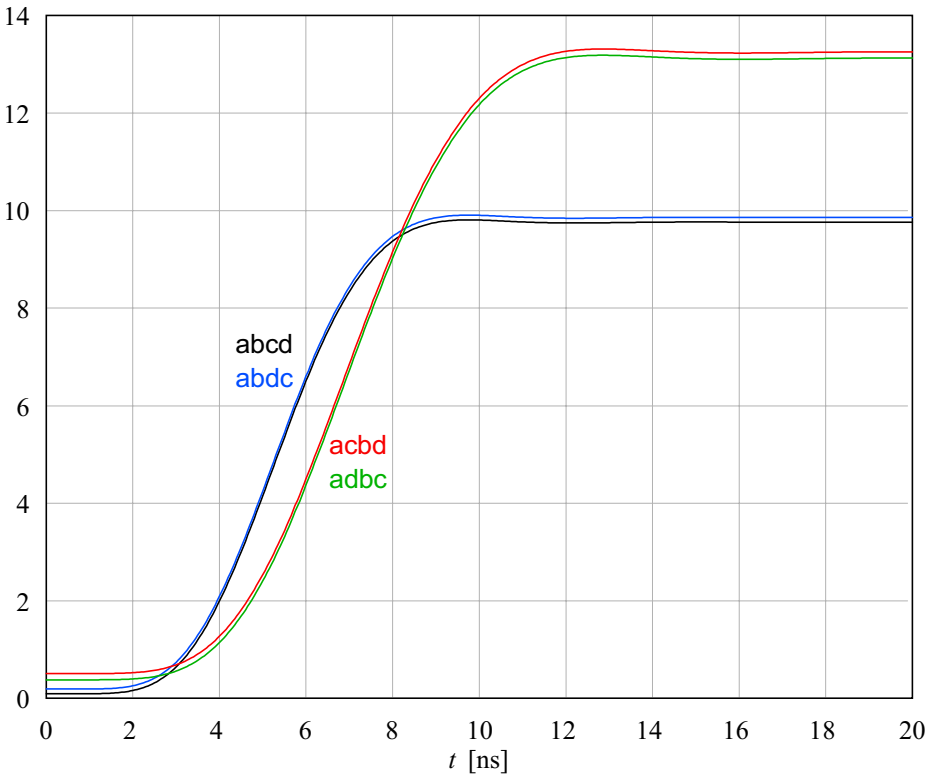

Fig. 5.1.9 : The slower responses of Fig. 5.1.8, when plotted with the actual gain, are actually those with a higher value of R_a and therefore a higher gain.

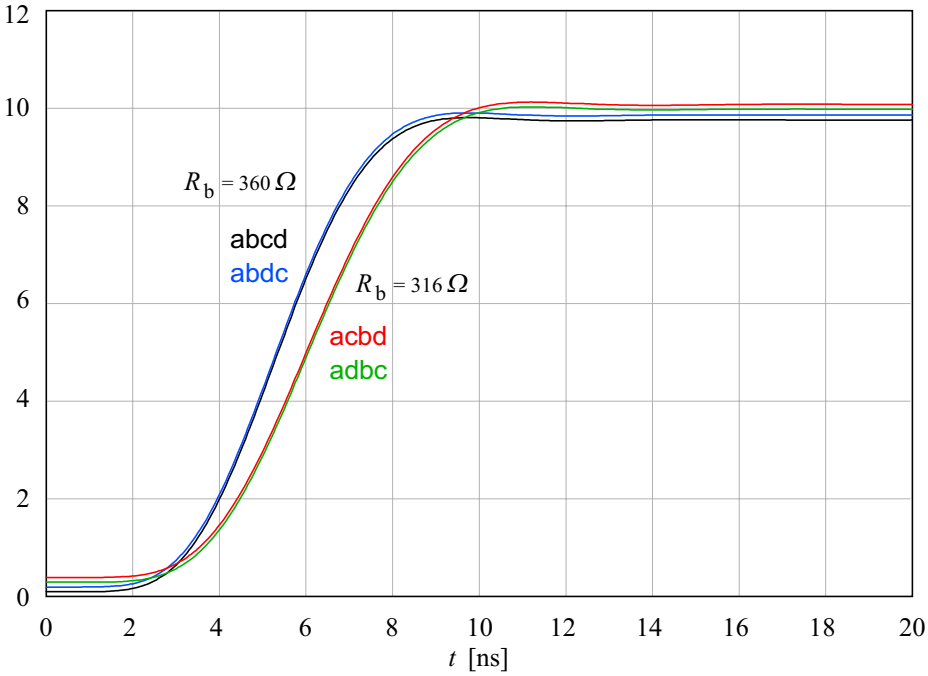

Fig. 5.1.10 : If the high-gain responses are recalculated by reducing R_b from the original 360 Ω to 316 Ω, the gain is equal in all four cases, However, those pole assignments, which put the poles with the higher imaginary part at the output stage, still result in a slightly slower system.

Table 5.1

R_b [Ω]	360	360	360	360	316	316
pole order :	abcd	abdc	acbd	adbc	acbd	adbc
A_0	9.667	9.667	12.74	12.74	9.817	9.817
R_a [Ω]	268.5	286.5	353.9	353.9	310.7	310.7
C_c [pF]	4.173	2.177	2.870	7.249	2.870	7.249
C_d [pF]	5.838	11.19	14.75	5.838	14.75	5.838
C_{bb} [pF]	0.779	0.779	1.201	1.201	1.201	1.201
C_{bd} [pF]	1.851	1.222	1.045	1.851	1.045	1.851
L_b [μH]	1.426	1.426	1.426	1.426	1.098	1.098
L_c [μH]	0.153	0.080	0.162	0.410	0.125	0.316
L_d [μH]	0.421	0.807	1.847	0.731	1.423	0.563
k_b	0.558	0.558	0.392	0.392	0.392	0.392
k_d	− 0.118	0.392	0.558	− 0.118	0.558	− 0.118

Table 5.1 : Circuit components for 4 of the 6 possible pole assignments. The last two columns represent the same pole assignment as the middle two, but have been recalculated for $R_b = 316\,\Omega$ and nearly equal gain. The first column is the example calculated in the text and its response is one of the two fastest. The other fast system (second column) is probably non-realizable (in discrete form), due to $C_c \approx 2$ pF. The last column (adbc) is, on the other hand, only slightly slower, but probably much easier to realize (T-coil coupling and the capacitance values).

In Table 5.1 we have collected all the design parameters for the four out of six possible pole assignments. The systems in the last two columns have the same pole assignments as in the middle two, but have been recalculated from a lower R_b value, in order to obtain the total voltage gain nearly equalto the first system. From a practical point of view, the first and the last column are the most interesting : the system represented by the first column is the fastest (as the second one, but the later is difficult to realize, mainly due to low C_c value), while the last one is only slightly slower but much easier to realize, mainly due to a lower magnetic coupling k_b and the non-problematic values of C_c and C_d .

The main problem of the first column system is the relatively high magnetic coupling factor of the output T-coil, k_b. A possible way to improve this could be by applying a certain amount of emitter peaking to either Q_1 or Q_3 emitter circuit. But then, we would get a 9-pole system and we would have to recalculate everything, which, by itself, is not a difficult task if we use the geometrical synthesis method, as we have seen. The problem with using emitter peaking would result from the required negative input impedance compensation and the associated stray capacitance of the compensating network.

A 9-pole system might be more easily implemented if, instead of the 3-pole section, we would use another L+T-coil 4-pole network. The real pole could then be provided by the signal source resistance and the Q_1 input capacitance, which we have chosen to neglect so far. With 9 poles, both T-coils can be made to accommodate those two pole-pairs with moderate imaginary part values (because the T-coil coupling factor depends only on the pole angle θ), so that the system bandwidth could be more easily maximized. A problem could arise with a low value of some capacitances, which might become difficult to achieve. But, as it is evident from Table 5.1, there are many possible variations (their number increases as the factorial of the number of

poles), so that a clever compromise can always be made. Of course, with a known signal source, an additional inductive peaking could be applied at the input, resulting in a total of 11 or maybe even 13 poles, but then the component tolerances and the adjustment precision would set the limits of realizability.

Finally, we would like to verify the initial claim that the input real pole s_1, due to the signal source and base spread resistance and the total input capacitance, can be neglected if it is larger than the system real pole s_a. Since the input pole is separated from the rest of the system by the first cascode stage, it can be accounted for by simply multiplying the system transfer function by it. In the frequency response, its influence is barely noticeable. In the step-response, Fig. 5.1.11, it affects mostly the envelope delay and the overshoot, while the risetime (in accordance with the frequency response) remains nearly the same.

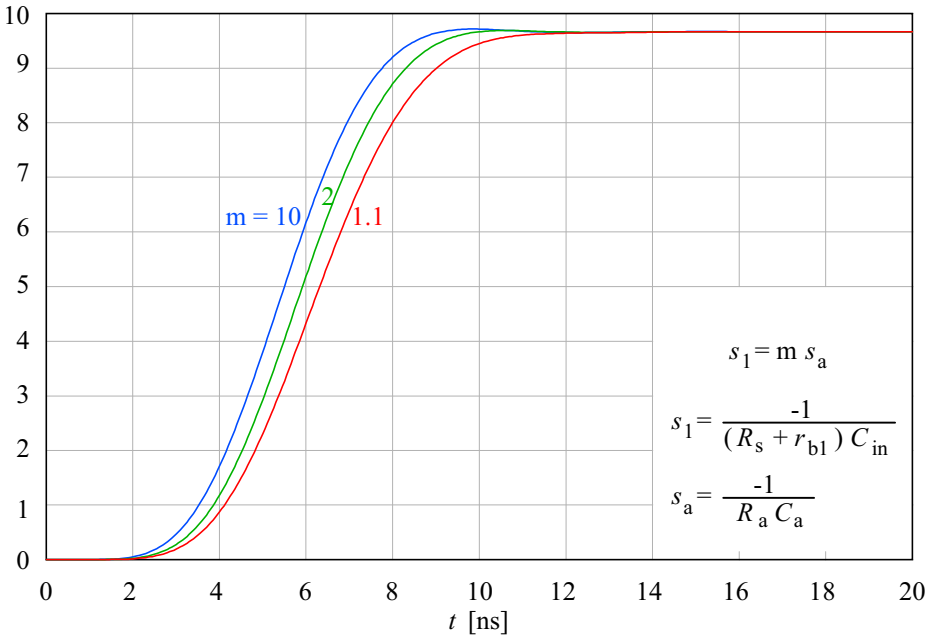

Fig. 5.1.11 : If the real input pole s_1 is at least twice as large as the system real pole s_a, its influence on the step response can be seen merely as an increased envelope delay and a reduced overshoot, while the risetime remains nearly identical.

Usually, the signal source impedance is 50 Ω or less. With an input capacitance of a few pF, the input pole can easily be several times larger than the system real pole. However, in most oscilloscopes an input buffer stage, with variable gain/attenuation, takes care of adapting the signal amplitude to the required level. Then, its output impedance, seen by the input capacitance of our amplifier, can be high enough that we would be forced to account for it. In such cases, as already stated before, it might become feasible to replace the 3-pole peaking network by another 4-pole L+T-coil network and make the input pole the main system real pole.

As already mentioned, the high capacitance of the CRT vertical deflection plates is the dominant cause of bandwidth limitation. The most advanced CRTs from the analog 'scope era have the deflection plates broken into a number of sections, connected externally by a series of T-coils, thus reducing the capacitance seen by the amplifier to just a fraction of the original value. In the same time, the T-coils provide a delay required to match the signal propagation to the electron velocity in the writing

beam (finite travel time by the deflection plates and some non-negligible relativistic[1] effects), aiding to a better beam control.

[1] In vacuum, a homogeneous electric field of strength $E = V/l$, where V is the voltage potential between the anode and cathode and l is the field length (the distance between the anode and cathode), an electron emitted by the hot cathode will be accelerated at the rate :

$$a = \frac{F}{m_e} = \frac{q_e E}{m_e} = \frac{q_e V}{m_e l} \tag{F1}$$

where the electron charge q_e = -1.602 × 10^{-19} As, the electron (rest) mass $m_e = 9.1095 \times 10^{-31}$ kg.

By assuming a constant acceleration (from a homogeneous field), the final electron velocity, just before hitting the anode, or passing through a small hole in it, is calculated as :

$$v = \sqrt{\frac{2\, q_e V}{m_e}} \tag{F2}$$

Eq. F2 can be considered correct if the final velocity is small in comparison with the velocity of light, otherwise we must apply the Theory of Relativity. For an anode voltage of only 100 V, the above equation would give a velocity $v = 5.93 \times 10^6$ m/s, which is almost 2 % of the velocity of light, $c = 2.99792458 \times 10^8$ m/s ≈ 3×10^8 m/s. Usually, CRT anode voltage values range from 25 kV to 35 kV, resulting in final electron velocities of about $c/3$.

The Theory of Relativity, as formulated by *Albert Einstein* in 1905, predicts an increase of the mass of an accelerated object in comparison to its rest mass, in accordance with the relation :

$$m_r = m_0 \frac{1}{\sqrt{1 - \left(\frac{v}{c}\right)^2}} \tag{F3}$$

where m_r is the object relativistic mass, m_0 is the object rest mass, v is the object velocity and c is the velocity of light. According to this, the electron mass changes with v, but v also changes due to the acceleration enforced by the electric field, so we must calculate the final velocity and mass iteratively.

Once the electron goes through the anode, its velocity towards the screen remains constant. But when it enters the deflection plates, only the transversal velocity components change and the electron path is parabolic, then linear again between the deflection plates and the screen. Since the deflection voltages are relatively low (<100 V), we can use Eq. F2 to calculate the deflection (but now V is the voltage between the deflection plates) ; however, instead of the rest electron mass m_e, the relativistic mass must be used. The relativistic mass, which the electron has acquired from the acceleration in the anode-cathode field, is calculated by Eq. F3.

For example, if we assume the non-deflected electron velocity $v = c/3$, the electron would acquire a mass $m_r \approx 1.06\, m_e$. By taking this back into Eq. F2, the vertical velocity component would be lower by some 3 % and, to get the desired deflection, we would have to increase the deflection voltage by the same amount. This is corrected by simply increasing the amplifier gain.

A more difficult problem arises from the fact that the electron takes a finite amount of time to travel the deflection field. For a constant or a slowly changing field, this time does not have to be accounted for ; however, when the deflection potential changes by several volts per nanosecond, this time becomes important, because it would affect both the horizontal and vertical deflection. By assuming again $v = c/3$ and a deflection field length (in the anode to screen direction) $d = 5$ cm, the time which the electron would spend in the deflection field is :

$$t_d = \frac{3\, d}{c} = \frac{3 \times 5 \times 10^{-2}\ [\mathrm{m}]}{3 \times 10^8\ [\mathrm{m/s}]} = 0.5\,\mathrm{ns} \tag{F4}$$

and this time is equal to the risetime of a 700 MHz oscilloscope. Therefore, the amount of deflection, in both horizontal and vertical direction, would depend also on the signal slew-rate and not only on its amplitude, as it should.

This problem is solved by breaking the plates into several smaller sections and introducing an appropriate signal delay between them, so that the electron is being deflected by a nearly constant filed throughout the travel time.